2024

Detection and Diagnosis of Bacterial Pathogens in Urine Using Laser-Induced Breakdown Spectroscopy

E J. Blanchette
University of Windsor

E A. Tracey
University of Windsor

A Baughan
University of Windsor

G E. Johnson
University of Windsor

H Malik
University of Windsor

See next page for additional authors

Spectrochimica Acta Part B: Atomic Spectroscopy 216 (2024) 106944

Contents lists available at ScienceDirect

Spectrochimica Acta Part B: Atomic Spectroscopy

journal homepage: www.elsevier.com/locate/sab

Detection and diagnosis of bacterial pathogens in urine using laser-induced breakdown spectroscopy

E.J. Blanchette [a], E.A. Tracey [a], A. Baughan [a], G.E. Johnson [a], H. Malik [a], C.N. Alionte [a], I.G. Arthur [b], M.E.S. Pontoni [a], S.J. Rehse [a,*]

[a] Department of Physics, University of Windsor, 401 Sunset Ave, Windsor, ON N9B 3P4, Canada
[b] Department of Biomedical Sciences, University of Windsor, 401 Sunset Ave, Windsor, ON N9B 3P4, Canada

ARTICLE INFO

Keywords:
Infection diagnosis
Bacteria
Laser-induced breakdown spectroscopy
Urine
UTI
Artificial neural network

ABSTRACT

The presence of bacterial cells from three species has been detected in clinical specimens of human urine using laser-induced breakdown spectroscopy (LIBS) by using a partial least squares discriminant analysis (PLS-DA) of 360 spectra obtained from 12 specimens of infected urine and 239 spectra obtained from eight specimens of sterile urine. Nominally sterile urine specimens obtained from four patients at a local hospital after being screened negative for the presence of bacterial pathogens were spiked with known aliquots of *Escherichia coli*, *Staphylococcus aureus*, and *Enterobacter cloacae* to simulate clinical urinary tract infections. Fifteen emission line intensities measured from the LIBS spectra and 92 ratios of those line intensities were used as 107 independent variables in the PLS-DA for discrimination between bacteria-containing specimens and sterile specimens. The PLS-DA models possessed a 98.3% sensitivity and a 97.9% specificity for the detection of pathogenic cells in urine when single-shot LIBS spectra were tested. To increase the signal to noise ratio, thirty spectra acquired from a single specimen were also averaged together and the averaged spectra were used to construct a model. When each averaged spectrum was withheld from the model individually for testing, the diagnostic test possessed a 100% sensitivity and a 100% specificity for the detection of bacterial cells in urine, although the number of test spectra was necessarily reduced.

The entire LIBS spectrum from 200 nm – 590 nm was input into an artificial neural network analysis with principal component analysis pre-processing (PCA-ANN) to diagnose the bacterial species once detected. This PCA-ANN test possessed an overall sensitivity of 97.2%, an overall specificity of 98.6%, and an overall classification accuracy of 97.9% when using 80% of the data to build a model and withholding 20% for cross-validation testing. The PCA-ANN was also performed on each of the 12 bacteria-containing filters individually, using the other 11 filters to build the model. The average sensitivity of this test, calculated by averaging the sensitivities measured for each of the three bacterial species, was 70.9% and the average specificity was 85.5%. Based on these results, the average classification accuracy for the test when used to discriminate between the three microorganisms was 80.6%. These results indicate the potential usefulness of LIBS for rapidly detecting and possibly diagnosing urinary tract infections in a clinical setting.

1. Introduction

Hospital acquired infections (HAI), or nosocomial infections, affect millions of people a year and are often antibiotic resistant, causing them to be one of the most common complications associated with hospital care [1]. Nosocomial infections can result from open surgical sites, catheters, or intubation with a ventilator and because of this, the most common infections are urinary tract infections (UTI), surgical infections, blood-stream infections (septicemia), and lower respiratory infections (pneumonia). Nosocomial infections are one of the leading causes of death and hospitals must screen patients for the presence of any nosocomial infection before discharging them [2]. The necessity of these screening tests requires the implementation of a rapid, sensitive, and specific diagnostic test capable of high-throughput with very low turn-

* Corresponding author.
E-mail addresses: etracey4@uwo.ca (E.A. Tracey), baughana@uwindsor.ca (A. Baughan), johnso53@uwindsor.ca (G.E. Johnson), malik72@uwindsor.ca (H. Malik), alionte@uwindsor.ca (C.N. Alionte), arthuri@uwindsor.ca (I.G. Arthur), pontonim@uwindsor.ca (M.E.S. Pontoni), rehse@uwindsor.ca (S.J. Rehse).

https://doi.org/10.1016/j.sab.2024.106944
Received 21 January 2024; Received in revised form 9 May 2024; Accepted 12 May 2024
Available online 14 May 2024

around time. This work will focus specifically on the development of a test suitable for detecting and diagnosing UTI using the technique of laser-induced breakdown spectroscopy (LIBS).

UTI are one of the most common infections in adult women, with up to 50% of women having experienced at least one UTI in their lifetime and upwards of 10% of women experiencing at least one UTI annually [3]. In 2007, UTI resulted in approximately 8.6 million health care visits in the United States with an estimated cost of 1.6 billion US dollars [4]. In addition to the prevalence in the population, UTI are also the most common nosocomial infection, with up to 80% of hospital-acquired UTI associated with the use of a bladder catheter [2]. Even a single catheterization can lead to UTI due to contamination of the catheter tip [5]. The gold standard for the diagnosis of UTI is a bacteriological urine culture, which must be performed shortly after acquiring the sample to avoid growth of other organisms [6]. Unfortunately, this culturing is often time consuming, costly, and is not capable of detecting all species of bacteria [7]. The threshold for the diagnosis of an active UTI is traditionally the measurement of 10^5 colony-forming-units (CFU) per mL of sample, but use of this number can result in significant rates of false negatives, with sensitivities possibly as low as 50% in some cases [8]. Complicating matters further, the prevailing understanding until very recently was that urine is a completely sterile fluid, but recent studies have called this into question stating that female patients contain bacterial colonies in the bladder [9]. This increases the need for a highly sensitive and specific test not just for detecting UTI, but also diagnosing the species of bacteria present in the urine to discriminate a patient's normal urinary microbiota from the pathogens associated with UTI.

The use of laser-induced breakdown spectroscopy for the detection and identification of bacterial pathogens has been well documented [10–13]. However the use of LIBS to detect or diagnose bacteria in urine has not been well studied [14]. Some authors have investigated the use of LIBS to investigate the chemical composition of urinary calculi in order to understand their formation and pathogenesis [15–17]. The ablation of the stony calculi presents a matrix more amenable to laser-ablation than the ablation of the liquid urine itself. Unfortunately, literature describing the use of LIBS for the direct analysis of urine specimens is also scant, with studies reported for the detection of cesium and the identification of diabetes mellitus [18,19].

This work describes preliminary studies investigating whether LIBS, when paired with a suitable chemometric or machine learning analysis, could be used as a point-of-care diagnostic technique directly on a fluid such as urine to test for the presence of UTI. The speed and specificity previously demonstrated by a LIBS-based diagnostic could aid in delivering more targeted treatment to patients which would reduce the overuse and abuse of broad-spectrum antibiotics in treating non-nosocomial UTI [20]. As well, the use of LIBS for screening patients before discharge from the hospital would improve the efficiency of the process, reducing time and the need for resources, while also freeing up much-needed hospital beds.

2. Materials and methods

2.1. Urine specimens

Sterile urine was provided by the pathology lab at the Windsor Regional Hospital for LIBS testing. All studies were done in accordance with the requirements of both the University of Windsor and Windsor Regional Hospital Research Ethics Boards. Specimens were completely anonymized prior to transfer and no information concerning patient identity, background, or demographics was provided. Such studies are classified as specimen transfers and are exempted from requiring a Research Ethics Board certificate according to both institutions. Only urine specimens that had already tested negative for bacterial infection were provided in these preliminary experiments and no other information of any sort was provided with the specimens. Urine specimens from four different patients were characterized to account for differences in patient physiology.

All urine specimens had typically been held by the hospital for at least five days before transfer for LIBS testing to allow for a negative bacterial culture result. The urine samples were stored in a refrigerator at 4 °C prior to testing. At the time of LIBS testing the urine specimens were anywhere from a week to several weeks old and it is possible that the LIBS spectra obtained from older specimens may not be representative of completely fresh specimens. Over time solute can coagulate and settle out of solution, however it is not thought this is a significant process from visible inspection of the specimens. All specimens were vortex-mixed prior to handling to insure the redistribution of any suspended particles. The diversity that was introduced by the use of specimens that were not the same age strengthens the conclusions of the work, as it served to increase the scatter in the data, which would be the realistic situation if the test were used to screen specimens from hundreds or thousands of unique patients. As the number of patient sources for the specimens utilized in this study was small, increasing the diversity in the collected data helped to simulate a more realistic model training set. No attempt was made in this study to analyze recently-obtained urine specimens from human participants.

2.2. Bacterial LIBS preparation

All urine specimens both with and without bacteria were prepared for LIBS testing by filtering and concentrating the fluid sample at the center of a nitrocellulose filter using a custom made centrifuge tube insert with an integrated concentration cone. This method for concentrating bacteria in fluid specimens at the center of a disposable filter has been described at length previously [21–23]. To achieve this concentration and deposition, a 3D-printed centrifuge insert was disassembled and a 9.5 mm diameter 0.45 μm pore size nitrocellulose membrane filter (HAWP04700, Millipore Inc.) was placed on the filter holder as shown in Fig. 1a. This pore size has been found to be adequate to catch the majority of bacterial cells during centrifugation. The centrifuge insert was then reassembled (Fig. 1b) and the aluminum concentration cone with a 1 mm open aperture at the apex (Fig. 1c) was placed into the insert. This cone attempts to force the fluid and bacteria to pass through the central 1 mm of the filter during centrifugation, concentrating the cells in that spot. The insert was then placed inside a 10 mL capacity centrifuge tube equipped with a hinged plastic cap, as shown in Fig. 1d. The pressure of the hinged cap acted to push the cone firmly into the nitrocellulose filter, providing a tight contact surface which retained most of the bacterial cells in the 1 mm deposition area in the center of the filter.

All urine specimens were vortex-mixed for several seconds and then 100 μL of urine was pipetted directly into the cone. The hinged plastic cap was then closed, sealing in all the liquid (Fig. 1e) and the entire assembly was centrifuged (PowerSpin BX C884, Unico) at 5000 rpm (2500 g's of force) for 5 min to deposit the urine on the filter. After centrifugation, the filter was removed from the centrifuge insert and mounted on a piece of steel with double sided sticky tape to hold it flat. This steel mounting piece was then inserted into the LIBS apparatus.

Colonies of *Escherichia coli*, *Staphylococcus aureus*, and *Enterobacter cloacae* were cultured on appropriate growth media and then removed from the solid medium plates. After triple washing to remove any residual nutrient media, the bacterial colonies were suspended in ultrapure megohmic water to reduce any background elemental contributions. Samples were assayed using optical densitometry to insure approximately equal concentrations of 10^8 colony forming units (CFU) per cubic centimeter of water were prepared for each species of bacteria. In most of the experiments described below dilutions of these standard suspensions were used to reduce the concentration to approximately 2×10^7 CFU/mL.

To create urine specimens that would simulate a UTI, the nominally-sterile urine specimens were ‘spiked’ with one of the bacterial species listed above. This was accomplished by pipetting bacteria and urine into the same cone to create a mixture of bacteria and urine. The centrifuge

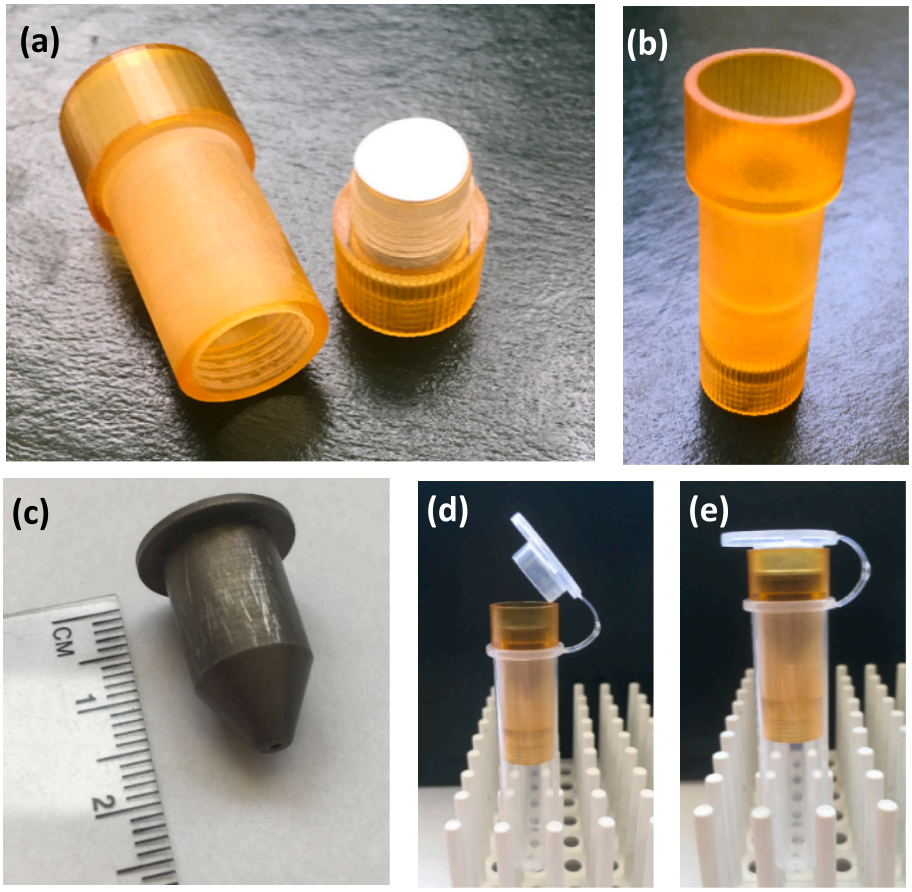

Fig. 1. The disassembled 3D printed centrifuge insert used for bacterial separation fitted with a 9.5 mm diameter disposable nitrocellulose membrane filter (a). The insert reassembled with the filter sealed in between the two sections (b). The aluminum cone with a 1 mm diameter aperture in the apex used to concentrate the bacteria in the center of the filter (c). The assembled apparatus inside a centrifuge tube prior to addition of urine (d) and the apparatus with the centrifuge tube cap closed after the addition of urine prior to centrifugation (e).

insert was re-assembled including filter and cone and 100 μL of a bacterial suspension was pipetted into the cone. Then, 100 μL of a sterile urine sample was pipetted into the same cone. This effectively creates a mixture of bacteria in urine. The apparatus was then centrifuged at 5000 rpm for 5 min just as the control samples were. After centrifugation, all of the bacterial cells in the initial urine suspension were deposited in a fairly uniform layer inside of a circular area with diameter of 1 mm, achieving a cell surface density of approximately 2.5×10^8 cells/cm^2. This deposition was confirmed by scanning electron microscopy and optical microscopy. The filters were then removed for LIBS testing.

2.3. LIBS apparatus

Once transferred to the LIBS ablation chamber, 30 single-shot LIBS spectra were acquired from the urine or bacteria/urine deposition. On one filter only 29 usable spectra were obtained. The ablation craters were approximately 75 μm in diameter and the spacing between adjacent ablation locations was approximately 150 μm. Knowing the bacterial cell surface density and the laser ablation spot size allows a calculation of approximately 11,000 cells ablated per laser shot, which is a low and clinically relevant number of cells for a common UTI. Deposition filters prepared in this way were ablated in an argon gas environment with an argon purge flow into the chamber of approximately 567 L/h (20 standard cubic feet per hour). The laser used for ablation was an Nd:YAG operating at 1064 nm (Quanta Ray LAB-150-10, Spectra Physics) with 10 Hz repetition rate, 10 ns pulse duration, and a pulse energy of 8 mJ/pulse at the target. The light from the plasma was collected by two matching parabolic aluminum mirrors (f = 5.08 cm, φ = 3.81 cm) and directed into a 1 m steel-encased multimodal optical fibre (numerical aperture = 0.22, core diameter = 600 μm).

The light from the plasma was dispersed by an echelle spectrometer (ESA 3000, LLA Instruments, GmbH) and detected by an intensified charge-coupled device (ICCD) camera. The echelle grating used in this experiment allowed a broadband spectrum from 200 to 840 nm to be collected with approximately 12 pm resolution in the ultraviolet wavelength range. The ICCD utilized a Kodak camera with a 2.54 cm × 2.54 cm CCD chip (1064 pixels by 1064 pixels, pixel size of 24 μm^2). The spectrometer was controlled by ESAWIN v3.20 software to set the delay time for data acquisition relative to the laser pulse (called the gate delay, τ_d) at 2 μs and the duration of spectral data acquisition (which is the camera exposure time, called the gate width, τ_w) at 20 μs for all bacterial experiments. This software also controlled the firing of the Nd:YAG laser Q-switch to provide nanosecond timing control.

2.4. Computerized data analysis: PLS-DA

The ESAWIN software measured the integrated area under the background-subtracted spectrum of 15 atomic/ionic emission lines from carbon, phosphorus, magnesium, calcium, and sodium. These 15 lines are shown in Table 1 and represent the elemental composition of the urine, bacterial cells, and the nitrocellulose filter medium. These lines were chosen specifically because they were reproducibly and consistently observed. No lines from any other elements (except for Stark-broadened hydrogen emission lines) were reliably observed.

To create more independent variables for the chemometric analysis

Table 1
Identification and wavelengths of the 15 strong emission lines consistently observed in the spectra of urine and urine spiked with bacteria.

Species	Wavelength nm
C I	247.856
P I	213.618
P I	214.914
P I	253.560
Mg II	279.079
Mg II	279.553
Mg II	279.806
Mg II	280.271
Mg I	277.983
Ca II	317.933
Ca II	393.366
Ca II	396.847
Ca I	422.673
Na I	588.995
Na I	589.593

of the spectra, ninety-two ratios of those line intensities were used with the 15 line intensities to create 107 independent variables for use in a partial least squares discriminant analysis (PLS-DA). The intent of the PLS-DA was to develop a model capable of discriminating between spectra obtained from sterile control urine samples and those spiked with bacteria. The identification of these 107 ratios is provided in the Supplementary Material Tables S1 and S2. The construction of simple ratios from the measured emission line intensities follows an approach applied successfully by Gottfried et al. for the discrimination of highly similar LIBS spectra acquired from explosive residues [24,25]. The choice of which lines to use and which ratios to construct to provide optimal spectral discrimination when using a chemometric algorithm such as PLS-DA or discriminant function analysis (DFA) was investigated by us previously in a non-urine bacterial system [26]. What was concluded in that study and in the other references was that having more independent variables allowed for more variance in the data to be expressed, which resulted in a better statistical classification of unknown spectra. These studies demonstrated that this approach was statistically superior to alternate approaches that did not combine the measured line intensities into ratios or approaches which attempted to combine all the emission lines measured from a given atomic species into one independent variable representing the overall intensity of that atomic species. Importantly, Putnam et al. observed that ratios should not be constructed blindly, but that that prior knowledge of which elemental lines contributed most significantly to accurate classification would allow the construction of the most appropriate ratios for accurate classification [26].

Once defined as belonging to one of two classes (either sterile control urine or urine with bacteria) the 107 independent variables from each spectrum were input into a PLS-DA algorithm implemented by the PLS_toolbox v.8.7.1 (Eigenvector Research, Inc.) running under Matlab 2016b v.9.1 PLS-DA is a variation of the partial least squares regression (PLS) algorithm. PLS regression constructs a linear regression model to predict a dependent variable from a set of known independent variables and in the specific utilization of PLS-DA, the dependent variable is actually the class (or identity) of the test data set, rather than a concentration or some other parameter. PLS-DA constructs a small number of latent variables (LVs) from the independent variables and these LVs are used to calculate the most probable class membership of an unknown test data set. In the PLS_toolbox, the number of LVs can be adjusted manually or can be assigned automatically by the program. For the bacterial discrimination described here, four or five LVs were suggested by the software and were sufficient to allow discrimination while avoiding overfitting of the data. The 107 variable datasets were always pre-processed by mean-centering and setting the standard deviation of each of the column of variables to one, a standard pre-processing step the PLS_toolbox refers to as "auto-scaling."

PLS-DA was also performed on data sets where all the spectra on a given filter were averaged together to increase the signal to noise ratio of the data. This averaging was achieved in two ways. In the first method, the average of each line was calculated in Microsoft Excel after the ESAWIN software had measured and exported the intensities of the 15 emission lines. In the second method, the CCD camera images were averaged in the ESAWIN software prior to the measurement of the 15 line intensities. In both these analyses, the 107 independent variable were again created from the averaged spectrum. These tests necessarily possessed far fewer data, only 12 bacterial spectra and 8 control urine spectra, as only that many filters were tested. Due to the improved quality of the data and the reduction in the number of datasets, typically only one LV was required for complete discrimination of the urine with bacteria from the sterile urine, accounting for approximately 85% of the variance in the data.

2.5. Computerized data analysis: PCA-ANN

To classify the three bacterial species present in the urine, an artificial neural network (ANN) was trained on a subset of the entire LIBS spectrum from 200 nm – 590 nm. The ANN was developed in Python with the libraries *Pandas*, *Numpy*, *Tensorflow*, *keras*, and *Scikit-Learn* and was run on a standard desktop PC using an Intel i9 CPU. To reduce the dimensionality of the data, the 42,000 variable spectra were first pre-processed with an unsupervised principal component analysis (PCA). Others have reported improved results when conducting a principal component analysis on LIBS data first and using the principal component scores as independent variables in an ANN [27,28]. The number of principle component scores retained from the PCA becomes the new number of input nodes in the ANN algorithm, significantly reducing training time. A PCA algorithm was developed in python using the libraries *sklearn.decomposition*, *pandas*, *numpy*, and *mpl_toolkits*. Ten PC scores which captured approximately 99% of the variance were kept for use in the ANN. Initially the data was mean-centered prior to PCA by calculating the mean of the data across each wavelength and subtracting the mean from each data point of the same wavelength. While mean-centering provided good results, they were no better than the results without the use of pre-processing. For all the results provided below the spectra data were not pre-processed prior to PCA.

An ANN optimization algorithm was developed to optimize a number of parameters in the ANN including the patience and number of hidden nodes utilized during algorithm training. The patience is a parameter that assists in the convergence of the algorithm by determining when the iterations of the model construction should cease if no improvement of the model performance can be achieved. The hidden nodes are the actual "neurons" connected in the neural network where the weighted input variables into the algorithm (the ten PC scores) are mapped onto the desired output variables (the bacterial classes.) This algorithm calculated the average sensitivity and specificity of the model for each value of patience and number of hidden nodes, allowing the algorithm parameters to be tailored to the bacterial spectral data. In all analyses only one hidden layer was used in the ANN. Before the data was classified with ANN, the program randomly split all the data up into a training set and a testing set. The testing set was created by removing 20% of the spectra from the data set. Typically in ANN, the larger the training set the better the performance, thus the use of this 80:20 cross-validation scheme. To represent a more realistic test, the data were tested in an "external validation" scheme, where all of the shots on a single filter were withheld entirely from the model and used as test data. Twelve individual tests (four filters from each of the three bacterial species) were then performed to obtain the classification accuracy for each species of bacteria. In addition, each test was repeated ten times in a row to account for variations in the convergence of the ANN. Variations in repeated results were observed due to the sensitivity of the ANN model construction to its initialization, and this is described in Section 3.4. The

sensitivities and specificities for each filter and species were constructed by averaging the results of the ten repetitions for each filter. Thus 120 PCA-ANN tests were performed on the data. Lastly, to demonstrate that the ANN was not fitting noise, experiments were performed where the spectral identities were randomized after PCA but before the PC scores were input to the ANN. During these tests no classification of the spectra was possible due to the lack of any variance between the now-randomized groups. Further details of the PCA-ANN are provided elsewhere [29].

3. Results and discussion

Fig. 2 shows a spectrum of *E. cloacae* bacteria deposited in urine with a spectrum of urine overlaid to show the difference between the two. Although qualitatively similar, calcium line intensities in the bacterial spectra were consistently higher than in the spectra from urine alone, magnesium line intensities were also consistently higher, and in this example, the sodium emission intensity was stronger in the control spectrum (although this was not consistently true for all combinations of specimens). Most notably, the phosphorus line in the spectra from bacteria in urine was larger than in the spectra from control urine, which served to indicate the presence of bacteria. The argon emission peaks originate from the presence of the buffer gas used during ablation, and were ignored. The strong carbon emission present in both spectra is predominantly, although not entirely, due to ablation of the nitrocellulose filter medium upon with the fluid specimens are deposited [30]. In Fig. 2 each spectrum is the average of thirty laser shots taken across an entire filter to increase the signal to noise of the spectra to allow a clear presentation of all the significant spectral features.

Despite the differences in emission intensities in the two spectra, the qualitative similarity of the spectra necessitated the use of the PLS-DA for discrimination, as described in Section 2.4. Other than the very weak phosphorus emission, no new lines were observed or measured in the bacterial spectra which would serve as a rapid and easy marker for the presence of bacteria. As the bacterial titer is further decreased, the quantitative difference between these two types of spectra will also decrease, requiring a multivariate analysis like PLS-DA that considers the relative intensities between all the independent variables, not just the intensity of a single emission line. In a similar manner, all of the bacterial spectra appear to be highly similar to each other, so no figure comparing the spectra from the various bacterial species is presented here. The bacterial spectrum in Fig. 2 is representative of the appearance of all the spectra collected. It is this high degree of similarity amongst the spectra from the various classes that requires the use of a

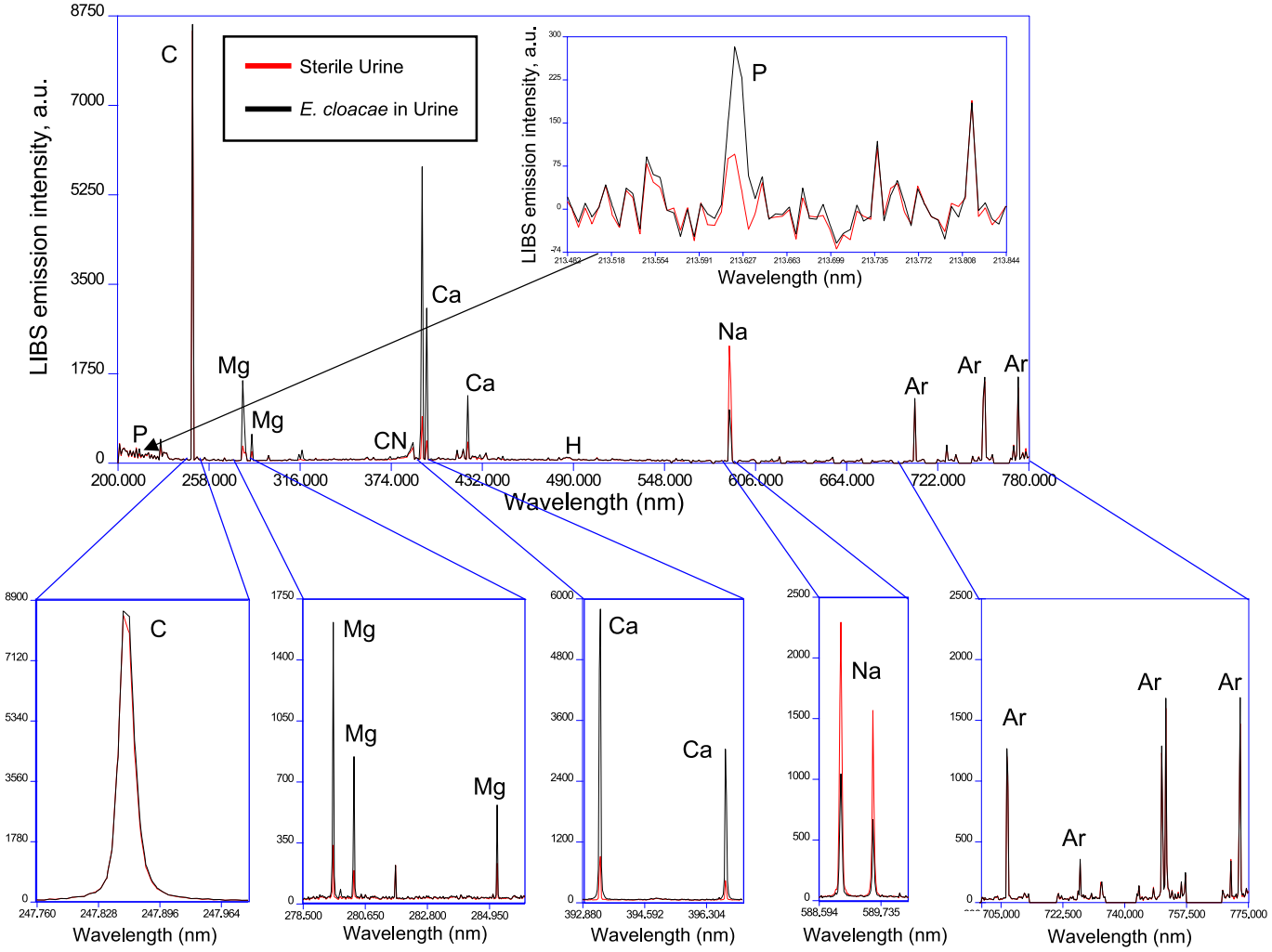

Fig. 2. Overlaid spectra of *Enterobacter cloacae* bacteria mixed with urine (black) and sterile urine (red). The spectra were dominated by the emission from calcium, magnesium, sodium, and carbon, shown below the full spectrum. Lines of phosphorus, although small, were consistently observed. Phosphorus emission (as shown in the inset) was never observed in the absence of bacteria, making it an indicator of the presence of bacterial cells. Argon was observed from the buffer gas used during ablation and was not included in any chemometric analysis. Specific emission line identities used in the analysis of these spectra are provided in Table 1. (For interpretation of the references to colour in this figure legend, the reader is referred to the web version of this article.)

multivariate analysis even more sophisticated than the PLS-DA and which motivated the initial investigation into the use of a PCA-ANN analysis of the entire LIBS spectrum. While not obvious to the eye, the subtle and reproducible differences in the spectra can be reliably identified and utilized by the model constructed in the ANN. The necessity of this machine learning approach (using e.g. an artificial neural network, a support vector machine, gradient boosting, k-nearest neighbors analysis, random forest, etc.) has been widely discussed for the analysis of LIBS data and is particularly important for the discrimination of biological targets which tend to exhibit a high degree of self-similarity [31,32].

3.1. PLS-DA on single-shot spectra

The PLS-DA was performed as described in Section 2.4 on the four filters of *S. aureus*, four filters of *E. coli*, four filters of *E. cloacae*, and eight filters of unspiked urine. A total of 20 tests were conducted. In each test all the spectra obtained from a single filter were withheld and tested against a model constructed from the remaining 19 filters classified as either "bacteria" or "no bacteria." After recording the classification results of the 30 spectra from this withheld filter, this filter was then reinserted into the dataset, a different filter was withheld for testing, and a new model constructed. This process was repeated sequentially until each filter had been tested individually against a new model constructed from all other filters. The results of these tests are show in in Table 2. Sterile Urine Filter #5 only had twenty-nine useable spectra, which in no way impacted the results.

For the 12 filters with bacteria-containing urine depositions, the fraction of the 30 single-shot LIBS spectra that classified as bacteria were used to calculate a sensitivity for that filter. The measured sensitivity for each filter is given in Table 2. The sensitivity is the fraction of spectra from a bacteria-positive sample that are classified by the model as a positive test result, which is called a true positive. The optimal medical test would have a sensitivity, or true positive rate, of 100%.

Because the 12 bacteria-containing filters were all positive for bacteria, no rates of false positives from these data could be used to calculate a specificity. The results of the 8 sterile urine filters were used to calculate the test's specificity. For the 8 filters with sterile urine depositions, the fraction of the 30 single-shot LIBS spectra that classified as urine (not bacteria) were used to calculate a specificity for that filter. The measured specificity for each control urine filter is given in Table 2. The specificity is the true negative rate of the test and is the fraction of the spectra from bacteria-negative filters that were classified by the model as a negative test result. The optimal medical test would have a specificity of 100%, meaning that no bacteria-negative samples would be diagnosed as bacteria-positive.

Averaging the measured sensitivities for the 12 bacteria filters yielded an overall sensitivity of 98.3% for this urine test and averaging the specificities for the 8 urine filters yielded an overall specificity of 97.9% when approximately 11,000 bacterial cells were ablated per laser shot.

3.2. PLS-DA on averaged spectra

Table 2 also shows the results of PLS-DA when all the spectra on a given filter were averaged together to increase signal to noise as described in Section 2.4. Both methods of averaging the spectra yielded a sensitivity of 100% and a specificity of 100%, with no filters being misclassified. Due to the averaging together of multiple spectra, this improved result now occurs due to the fact that approximately 330,000 total bacterial cells were ablated for each test. This is still a clinically relevant number of cells. Although there were far fewer data in the model and thus far fewer results due to the averaging, it is believed that this way of analyzing the data will ultimately be of clinical utility, as the specimen contributed by a single patient must yield a single diagnosis to the physician, not thirty, to allow the initiation of appropriate therapy. The best method for interpreting and relaying the results of tests such as those presented in Table 2 is still being studied, however it is apparent that the analysis of single-shot spectra and averaged spectra both can provide high sensitivities and specificities when this number of bacterial cells is analyzed.

Table 2
The results of 20 PLS-DA tests performed on filters of bacteria-containing urine and sterile urine.

Filter Identity	Sensitivity %	Specificity %	Averaged Result (Excel)[a]	Averaged Result (ESA)[b]
S. aureus + Urine Filter #1	100	–	Bacteria	Bacteria
S. aureus + Urine Filter #2	100	–	Bacteria	Bacteria
S. aureus + Urine Filter #3	96.67	–	Bacteria	Bacteria
S. aureus + Urine Filter #4	100	–	Bacteria	Bacteria
E. coli + Urine Filter #1	100	–	Bacteria	Bacteria
E. coli + Urine Filter #2	100	–	Bacteria	Bacteria
E. coli + Urine Filter #3	100	–	Bacteria	Bacteria
E. coli + Urine Filter #4	100	–	Bacteria	Bacteria
E. cloacae + Urine Filter #1	93.33	–	Bacteria	Bacteria
E. cloacae + Urine Filter #2	90	–	Bacteria	Bacteria
E. cloacae + Urine Filter #3	100	–	Bacteria	Bacteria
E. cloacae + Urine Filter #4	100	–	Bacteria	Bacteria
Sterile Urine Filter #1	–	100	No Bacteria	No Bacteria
Sterile Urine Filter #2	–	96.67	No Bacteria	No Bacteria
Sterile Urine Filter #3	–	93.33	No Bacteria	No Bacteria
Sterile Urine Filter #4	–	100	No Bacteria	No Bacteria
Sterile Urine Filter #5	–	93.10	No Bacteria	No Bacteria
Sterile Urine Filter #6	–	100	No Bacteria	No Bacteria
Sterile Urine Filter #7	–	100	No Bacteria	No Bacteria
Sterile Urine Filter #8	–	100	No Bacteria	No Bacteria

[a] refers to the averaging of spectral line intensities in MS Excel after measurement and extraction by the ESAWIN software.
[b] refers to the averaging of spectral line intensities on the CCD chip by the ESAWIN software prior to the measurement of emission line intensities.

3.3. PCA-ANN on full-spectrum data: 80:20 cross-validation

Table 3 shows the results of the full-spectrum PCA-ANN performed on all of the spectra obtained from the 12 filters with bacteria-containing urine utilizing an 80:20 cross-validation as described in Section 2.5. No sterile urine spectra were included in this model. In this table, sensitivity

Table 3
Full-spectrum PCA-ANN results using the spectra from 12 filters of bacteria-containing urine tested with an 80:20 cross-validation.

	Bacterial Identity		
	S. aureus	*E. coli*	*E. cloacae*
Sensitivity	100%	100%	91.67%
Specificity	100%	95.83%	100%
Classification Accuracy	100%	97.91%	95.83%

measures the percentage of bacteria spectra correctly classified, (e.g. an *S. aureus* sensitivity of 100% means that all individual *S. aureus* spectra were correctly classified as belonging to the *S. aureus* class, a true positive) while specificity measures the percentage of spectra that did not belong to that class that were correctly classified as not belonging to the class, (e.g. an *S. aureus* specificity of 100% means that none of the spectra from either of the other two classes were incorrectly classified as belonging to the *S. aureus* class, which would have been a false positive.)

For an optimal medical test, the sensitivity and specificity should be optimized to the highest values they can be without compromising the accuracy of one value in favor of the other. Ideally, the sensitivity and specificity for a medical test should both be 100%, but typically there are no realistic medical tests that achieve this level of accuracy. The focus is on achieving a balance between the two values. To summarize the overall performance of a medical test, classification accuracy is the metric used, which is defined as the fraction of predictions a model or test got right out of the total number of predictions. This can be summarized as: $classification\ accuracy = \frac{TP+TN}{TP+TN+FP+FN} \times 100\%$. These values are shown in Table 3 for each species tested. Averaging the results for the three bacterial species yielded an overall test sensitivity of 97.2%, an overall specificity of 98.6%, and an overall classification accuracy of 97.9%.

3.4. PCA-ANN on full-spectrum data: external validation

To provide a more realistic test, 120 PCA-ANN tests were run by performing ten repetitions of 12 models. Each model was constructed by withholding all the spectra acquired on a single unique filter and then constructing a PCA-ANN model from all the spectra from the other 11 filters. The spectra from the withheld filter were then classified by this model, as described in Section 2.5. Table 4 shows the results of this full-spectrum PCA-ANN tested in this way. In this test, the sensitivities and the specificities were acquired by averaging over each of the ten repetitions. The results for each test are provided in the Supplementary Material in Tables S3 through S5. Table 4 also provides the overall test sensitivity, specificity, and classification accuracy obtained by averaging the values obtained for each of the three species.

It is not surprising that the results shown in Table 4 are less accurate than the results presented in Table 3. This is a result of the more realistic testing of the model. In the 80:20 cross-validation, the model and test data were randomized from all of the spectral data sets. It is expected that 80% of the spectra from any given filter were included in the model, making it significantly easier to identify unclassified spectra from the other 20% of the spectra from that filter. The external validation is much more realistic because it incorporates possible variations in sample preparation, day-to-day variations in the LIBS apparatus, true differences in the urine obtained from different patients used for the tests on different days, etc. It is anticipated and observed that the variance between spectra obtained from a single filter (all obtained at the same time) was smaller than the variance between spectra from different filters which were often taken days or weeks apart and were obtained from different patients. The decrease in model performance was thus anticipated, but this methodology provides a more accurate determination of the test's overall accuracy. The overall test sensitivity, specificity, and classification accuracy were calculated by averaging the values obtained from each species and are shown in Table 4. Final values of 70.9%, 85.5% and 80.6% respectively were obtained. These results are all statistically lower than similar tests conducted on the same species spiked into blood specimens [29]. It is likely that the higher concentration of salts and other elements in the urine, as compared to blood, yielded a LIBS spectrum that was more similar to the bacteria spectra that what occurred in blood. This will need to be studied more extensively on spectra obtained from a wider diversity and a greater number of patients.

Table 4
Full-spectrum PCA-ANN results using the spectra from 12 filters of bacteria-containing urine tested with an external validation (entire filters withheld from the model sequentially).

	Bacterial Identity		
	S. aureus	*E. coli*	*E. cloacae*
Sensitivity	86.9%	63.6%	62.3%
Specificity	85.9%	87.7%	82.8%
Classification Accuracy	86.3%	79.7%	76.0%
Overall Test Sensitivity	70.9%		
Overall Test Specificity	85.5%		
Overall Test Classification Accuracy	80.6%		

The necessity of performing ten PCA-ANN repetitions of the test are made obvious by looking at the scatter of the ten results obtained from each filter (shown in Supplementary Material Tables S3 through S5). The scatter is a result of the stochastic nature of ANN model building, as opposed to the deterministic construction of a chemometric model such as PLS-DA, which is essentially a linear algebra calculation. The construction of an ANN model can be sensitive to the initialization of the parameters, the order in which spectra are input to the model, the number of hidden layers, etc. In the work described here, the number of hidden layers was always kept at one. On one filter of *E. coli*, the sensitivity was measured to be 1.0 on one run (30 out of 30 spectra classified as *E. coli*) but was measured to be 0.27 on another run. It is believed that the quality of the data has much to do with this scatter, as in previous work performed while constructing these models, high-quality data were seen to exhibit some small amount of scatter in the classification results, but nowhere near this level. Work is ongoing to improve the quality of the LIBS data (by improving the signal-to-noise of the data and the shot-to-shot consistency of the spectra), as it has been determined that for the experiments performed here, it is the quality of the data, not the quality of the algorithm, that needs to improve to allow for more consistent and accurate classification.

It is also possible that the number and diversity of data available for model construction was not sufficient to achieve consistently high rates of accuracy. As specified, each filter of 30 spectra was tested against a model constructed from 11 other filters, or 330 spectra. Most likely, the model needs to be constructed from a much greater number of spectra as ANNs generally perform more accurately when the training datasets are large. These specimens should also be collected from a much greater number of patient donors to increase the intrinsic diversity within the training dataset, which tends to add robustness to the model's ability to classify spectra that deviate from the average representative spectra in the class. It is hoped that a larger and more diverse collection of specimens will be made available in the future.

Another issue that is being addressed is the performance of the concentration cone during the bacterial deposition. In both our previous work with blood and in this work, it was occasionally seen that entire filters of spectra would essentially fail to classify properly. It was typically these specific filters that contributed most strongly to a decline in the reported accuracy, rather than the overall lack of accuracy of the model. In blood, two of 19 filters tested performed extremely poorly, and in the work reported here one filter of *E. cloacae* was seen to perform poorly. Poor performance was indicated in this case by six of the ten test repetitions returning a sensitivity of zero (none of the 30 spectra on the filter were correctly classified as *E. cloacae*) and none of the test repetitions ever returning a sensitivity above 33.3% (only ten spectra out of the 30 acquired from the filter being correctly classified). Usually, visible inspection of the filters either pre- or post-ablation would give evidence of the quality of the deposition, indicated by the lack of a clearly visible concentration at the center of the filter. A close inspection of the LIBS data post-acquisition revealed anomalous behavior, all of the spectra being qualitatively different from the anticipated spectrum, or all being inordinately small, was typical in these cases. This indicated it was a failure to prepare the specimen properly, not a shot-to-shot failure of the LIBS technique or a failure of the model construction that was

responsible. Nonetheless, no mechanism for data-rejection is yet built into the current testing methodology, so all of this data was always included in all of the models and is reported in all results. It is possible that these anomalous filters are erroneously lowering the reported accuracy improperly, but until improvements to the sample preparation methodology can be made, the data from all these filters are included for completeness. Work is underway to construct and test a new centrifuge cone insert that is constructed in such a way that the seal between the cone apex and the filter is more reproducibly achieved, insuring that the bacteria are more reliably concentrated in a small area a millimeter in diameter at the center of the filter. It is hoped that this improvement will address these issues described here.

4. Conclusions

An investigation into the use of laser-induced breakdown spectroscopy (LIBS) in combination with appropriate machine learning techniques to analyze urine specimens for the purpose of detecting bacterial pathogens and identifying the species of those pathogens has been reported. Clinical specimens of urine were tested by spiking urine samples from four patients with known aliquots of three species of bacteria. A PLS-DA test using four or five latent variables was found to be adequate for discriminating sterile urine from the urine spiked with the known bacteria. The PLS-DA test possessed an overall sensitivity of 98.3% and an overall specificity of 97.9% for the detection of pathogenic bacteria in urine when 599 spectra from 20 filters were tested by removing one entire filter at a time from the model and testing each spectrum individually. In addition, this test was repeated with all the spectra obtained from a single filter averaged to enhance the signal to noise of the overall spectrum. In this case, 12 of 12 filters of infected urine tested positive and 8 of 8 filters with sterile urine tested negative, yielding 100% sensitivity and 100% specificity.

An artificial neural network with one hidden layer was constructed to classify the three pathogen species present in the spiked urine samples. A principal component analysis was performed on the entire LIBS spectrum to reduce the dimensionality of the data from 42,000 independent variables down to ten. The first ten principal component scores captured 99% of the variance in the data and were used as the input data to the ANN implemented with python on a standard desktop PC. A typical validation was done by performing an 80:20 split of the data, testing 20% of all available data (chosen randomly) against the remaining 80% of the data which was used to construct the model. Spectra tested in this way demonstrated an average sensitivity of 97%, an average specificity of 99%, and an average classification accuracy of 98%.

The model was also tested in a more realistic and appropriate manner by withholding one filter at a time from the model construction and then testing the spectra from that filter ten times sequentially to examine the variance in the results of the ANN performance. When the spectra were tested in this way, the overall test sensitivity, specificity, and classification accuracy were calculated by averaging the values obtained from each of the three bacterial species and final values of 70.9%, 85.5% and 80.6% respectively were obtained. Due to this averaging, one very poorly performing filter of *E. cloacae* was found to be responsible for a significant decrease in the overall sensitivity of the test when used with that microorganism, but all the spectra from that filter were retained in the analysis for completeness. Future investigations of the same methodology for the testing of blood specimens to develop a rapid diagnostic technology for treating septicemia (blood infection) and an investigation of the effect on decreasing the number of bacteria spiked into the urine are ongoing with a newly designed deposition apparatus that will increase the quality and the reproducibility of bacterial concentration on the filter medium.

CRediT authorship contribution statement

E.J. Blanchette: Writing – original draft, Visualization, Validation, Software, Methodology, Investigation, Formal analysis. **E.A. Tracey:** Validation, Investigation, Formal analysis. **A. Baughan:** Validation, Software, Investigation, Formal analysis. **G.E. Johnson:** Validation, Software, Investigation, Formal analysis. **H. Malik:** Validation, Investigation, Formal analysis. **C.N. Alionte:** Validation, Investigation, Formal analysis. **I.G. Arthur:** Validation, Investigation, Formal analysis. **M.E.S. Pontoni:** Validation, Software, Formal analysis. **S.J. Rehse:** Writing – review & editing, Writing – original draft, Visualization, Supervision, Project administration, Methodology, Funding acquisition, Conceptualization.

Declaration of competing interest

The authors declare that they have no known competing financial interests or personal relationships that could have appeared to influence the work reported in this paper.

Data availability

Data can be made available on request.

Acknowledgements

This work was supported by the Natural Sciences and Engineering Research Council (NSERC) of Canada under Grant award number RGPIN/05842-2017. We are grateful to the Windsor Regional Hospital, specifically Lucy DiPietro and Dr. Mohamed El-Fakharany for their assistance in obtaining the clinical urine specimens; to Ingrid Churchill who supplied the initial stabs for all bacterial cultures and provided advice and assistance with microbiological questions; and to Sharon Lackie who performed the measurements with the scanning electron microscope.

Appendix A. Supplementary data

Supplementary data to this article can be found online at https://doi.org/10.1016/j.sab.2024.106944.

References

[1] K. Chau, Knowledge attitude and practice towards infection control measures amongst medical students in a medical teaching tertiary care hospital, Int. J. Clin. Med. 8 (2017) 534–542, https://doi.org/10.4236/ijcm.2017.89050.
[2] World Health Organization, in: G. Ducel, J. Fabry, L. Nicolle (Eds.), Prevention of Hospital-Acquired Infections: A Practical Guide, 2nd ed, World Health Organization, Geneva, 2002, pp. 1–64.
[3] T.K. Price, E.E. Hilt, T.J. Dune, E.R. Mueller, A.J. Wolfe, L. Brubaker, Urine trouble: should we think differently about UTI? Int. Urogynecol. J. 29 (2018) 205–210, https://doi.org/10.1007/s00192-017-3528-8.
[4] S.M. Schappert, E.A. Rechtsteiner, Ambulatory medical care utilization estimates for 2007, Vital Health Stat. 13 (169) (2011) 1–38 (PMID: 21614897).
[5] J.M.T. Barfor, K. Anson, Y. Hu, A.R.M. Coates, A model of catheter-associated urinary tract infection initiated by bacterial contamination of the catheter tip, BJU Int. 102 (2008) 67–74, https://doi.org/10.1111/j.1464-410X.2008.07465.x.
[6] G. Schmiemann, E. Kniehl, K. Gebhardt, M.M. Matejczyk, E. Hummers-Pradier, The diagnosis of urinary tract infection, a systematic review, Dtsch. Arztebl. Int. 107 (2010) 361–367, https://doi.org/10.3238/arztebl.2010.0361.
[7] M. Barza, Urinary tract, in: N.C. Engleberg, V.J. DiRita, T. Dermody, M. Schaechter (Eds.), Mechanisms of Microbial Disease, 3rd ed, Lippincott Williams & Wilkins, 2007, pp. 564–572.
[8] C.M. Chu, J.L. Lowder, Diagnosis and treatment of urinary tract infections across age groups, Am. J. Obstet. Gynecol. 219 (2018) 40–51, https://doi.org/10.1016/j.ajog.2017.12.231.
[9] A.J. Wolfe, L. Brubaker, "Sterile urine" and the presence of bacteria, Eur. Urol. 68 (2015) 173–174, https://doi.org/10.1016/j.eururo.2015.02.041.
[10] V.K. Singh, A.K. Rai, Prospects for laser-induced breakdown spectroscopy for biomedical applications: a review, Lasers Med. Sci. 26 (2011) 673–687, https://doi.org/10.1007/s10103-011-0921-2.
[11] S.J. Rehse, H. Salimnia, A.W. Miziolek, Laser-induced breakdown spectroscopy (LIBS): an overview of recent progress and future potential for biomedical

applications, J. Med. Eng. Technol. 36 (2012) 77–89, https://doi.org/10.3109/03091902.2011.645946.
[12] V.K. Singh, J. Sharma, A.K. Pathak, C.T. Ghany, M.A. Gondal, Laser-induced breakdown spectroscopy (LIBS): a novel technology for identifying microbes causing infectious diseases, Biophys. Rev. 10 (2018) 1221–1239, https://doi.org/10.1007/s12551-018-0465-9.
[13] S.J. Rehse, A review of the use of laser-induced breakdown spectroscopy for bacterial classification, quantification, and identification, Spectrochim. Acta Part B 154 (2019) 50–69, https://doi.org/10.1016/j.sab.2019.02.005.
[14] Q.I. Mohaidat, K. Sheikh, S. Palchaudhuri, S.J. Rehse, Pathogen identification with laser-induced breakdown spectroscopy: the effect of bacterial and biofluid specimen contamination, Appl. Opt. 51 (2012) B99–B107, https://doi.org/10.1364/AO.51.000B99.
[15] B.B.S. Jaswal, V.K. Singh, Analytical assessments of gallstones and urinary stones: a comprehensive review of the development from laser to LIBS, Appl. Spectrosc. Rev. 50 (2015) 473–498, https://doi.org/10.1080/05704928.2015.1010206.
[16] K. Štěpánková, K. Novotný, M.V. Vašinová Galiová, V. Kanický, J. Kaiser, D. W. Hahn, Laser ablation methods for analysis of urinary calculi: comparison study based on calibration pellets, Spectrochim. Acta Part B 81 (2013) 43–49, https://doi.org/10.1016/j.sab.2012.12.009.
[17] J. Anzano, R.J. Lasheras, Strategies for the identification of urinary calculus by laser induced breakdown spectroscopy, Talanta 79 (2009) 352–360, https://doi.org/10.1016/j.talanta.2009.03.065.
[18] A. Metzinger, É. Kovács-Széles, G. Galbács, An assessment of the potential of laser-induced breakdown spectroscopy (LIBS) for the analysis of cesium in liquid samples of biological origin, Appl. Spectrosc. 68 (2014) 789–793, https://doi.org/10.1366/13-07.
[19] I. Rehan, S. Khan, M.A. Gondal, Q. Abbas, R. Ullah, Non-invasive diabetes mellitus diagnostics using laser-induced breakdown spectroscopy and support vector machine algorithm, Arab. J. Sci. Eng. (2023), https://doi.org/10.1007/s13369-023-08269-8.
[20] M.L. Grover, J.D. Bracamone, A.K. Kanodia, M.J. Bryan, S.P. Donahue, A.-M. Warner, et al., Assessing adherence to evidence-based guidelines for the diagnosis and management of uncomplicated urinary tract infection, Mayo Clin. Proc. 82 (2007) 181–185, https://doi.org/10.4065/82.2.181.
[21] D.J. Malenfant, A.E. Paulick, S.J. Rehse, A simple and efficient centrifugation filtration method for bacterial concentration and isolation prior to testing liquid specimens with laser-induced breakdown spectroscopy, Spectrochim. Acta Part B 158 (2019) 105629, https://doi.org/10.1016/j.sab.2019.05.018.
[22] A.E. Paulick, D.J. Malenfant, S.J. Rehse, Concentration of bacterial specimens during centrifugation prior to laser-induced breakdown spectroscopy analysis, Spectrochim. Acta Part B 157 (2019) 68–75, https://doi.org/10.1016/j.sab.2019.05.012.
[23] A.E. Paulick, Development of Laser-Induced Breakdown Spectroscopy as a Rapid Diagnostic Tool for Bacterial Infection, University of Windsor, Windsor, 2018. https://scholar.uwindsor.ca/etd/7653.
[24] J.L. Gottfried, F.C. De Lucia Jr., C.A. Munson, A.W. Miziolek, Standoff detection of chemical and biological threats using laser-induced breakdown spectroscopy, Appl. Spectrosc. 62 (2008) 353–363, https://doi.org/10.1366/000370208784046759.
[25] J.L. Gottfried, F.C. DeLucia Jr., C.A. Munson, A.W. Miziolek, Laser-induced breakdown spectroscopy for detection of explosives residues: a review of recent advances, challenges, and future prospects, Anal. Bioanal. Chem. 395 (2009) 283–300, https://doi.org/10.1007/s00216-009-2802-0.
[26] R.A. Putnam, Q.I. Mohaidat, A. Daabous, S.J. Rehse, A comparison of multivariate analysis techniques and variable selection strategies in a laser-induced breakdown spectroscopy bacterial classification, Spectrochim. Acta Part B 87 (2013) 161–167, https://doi.org/10.1016/j.sab.2013.05.014.
[27] Y. Zhao, Q. Wang, X. Cui, G. Teng, K. Wei, H. Liu, Discrimination of hazardous bacteria with combination laser-induced breakdown spectroscopy and statistical methods, Appl. Opt. 59 (2020) 1329–1337, https://doi.org/10.1364/AO.379136.
[28] Y. Yang, C. Li, S. Liu, H. Min, C. Yan, M. Yang, et al., Classification and identification of brands of iron ores using laser-induced breakdown spectroscopy combined with principal component analysis and artificial neural networks, Anal. Methods 12 (2020) 1316–1332, https://doi.org/10.1039/C9AY02443C.
[29] E.J. Blanchette, Detection and Diagnosis of Bacterial Pathogens in Blood and Urine Using Laser-Induced Breakdown Spectroscopy, University of Windsor, Windsor, 2022. https://scholar.uwindsor.ca/etd/9000.
[30] D.J. Malenfant, D.J. Gillies, S.J. Rehse, Bacterial suspensions deposited on microbiological filter material for rapid laser-induced breakdown spectroscopy identification, Appl. Spectrosc. 70 (2016) 485–493, https://doi.org/10.1177/0003702815626673.
[31] L.-N. Li, X.-F. Liu, F. Yang, W.-M. Xu, J.-Y. Wang, R. Shu, A review of artificial neural network based chemometrics applied in laser-induced breakdown spectroscopy analysis, Spectrochim. Acta Part B 180 (2021) 106183, https://doi.org/10.1016/j.sab.2021.106183.
[32] D. Zhang, H. Zhang, Y. Zhao, Y. Chen, C. Kea, T. Xu, et al., A brief review of new data analysis methods of laser-induced breakdown spectroscopy: machine learning, Appl. Spectrosc. Rev. 57 (2022) 89–111, https://doi.org/10.1080/05704928.2020.1843175.